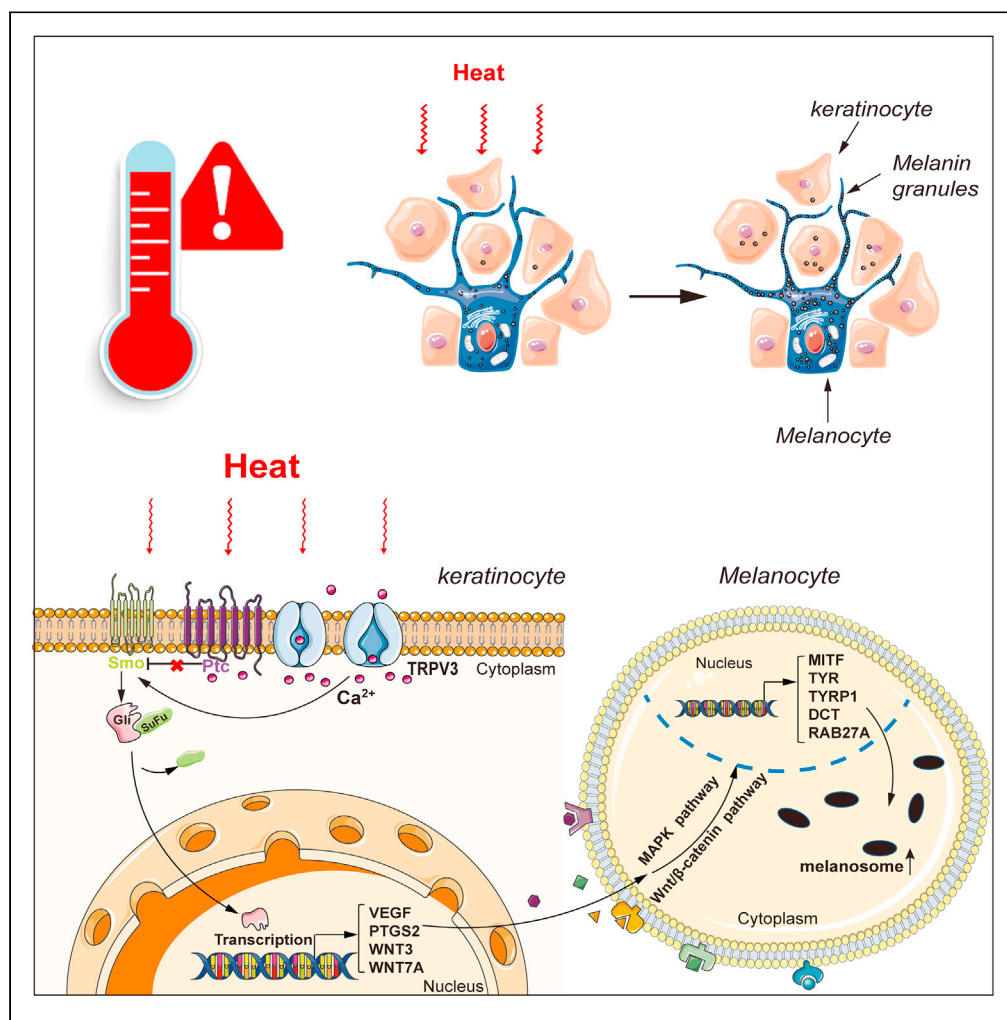


Article

Heat promotes melanogenesis by increasing the paracrine effects in keratinocytes via the TRPV3/ Ca^{2+} /Hh signaling pathway



Lan Zhang,
Hongliang Zeng,
Ling Jiang, ...,
Jinhua Huang,
Jing Chen,
Qinghai Zeng

zengqinghai@csu.edu.cn

Highlights

Heat promoted melanogenesis by increasing the paracrine effects in keratinocytes

Heat increased the paracrine effects in keratinocytes via the Hh signaling pathway

Heat-induced TRPV3-mediated Ca^{2+} influx activated the Hh signaling pathway



Article

Heat promotes melanogenesis by increasing the paracrine effects in keratinocytes via the TRPV3/Ca²⁺/Hh signaling pathway

Lan Zhang,¹ Hongliang Zeng,² Ling Jiang,¹ Chuhan Fu,¹ Yushan Zhang,¹ Yibo Hu,¹ Xiaolin Zhang,¹ Lu Zhu,¹ Fan Zhang,¹ Jinhua Huang,¹ Jing Chen,¹ and Qinghai Zeng^{1,3,*}

SUMMARY

Global warming and rising temperature significantly increase the incidence of heat stress, which is known to affect the process of inflammation and aging. However, the effect of heat stress on skin melanogenesis is not fully known. We found that healthy foreskin tissues underwent significant pigmentation when exposed to 41°C. Furthermore, heat stress promoted melanogenesis in pigment cells by increasing the paracrine effects of keratinocytes. High-throughput RNA sequencing showed that heat stress activates the Hedgehog (Hh) signaling pathway in keratinocytes. The agonists of Hh signaling promote the paracrine effect of keratinocytes on melanogenesis. In addition, transient receptor potential vanilloid (TRPV) 3 agonists activate the Hh signaling in keratinocytes and augment its paracrine effect on melanogenesis. The heat-induced activation of Hh signaling is dependent on TRPV3-mediated Ca²⁺ influx. Heat exposure promotes melanogenesis by increasing the paracrine effects in keratinocytes via the TRPV3/Ca²⁺/Hh signaling pathway. Our findings provide insights into the mechanisms of heat-induced skin pigmentation.

INTRODUCTION

Global warming has increased the risk of heat stress and related disorders, such as maternal health and neonatal outcomes,¹ as well as cardiovascular and respiratory complications.² Heat stress can also cause skin aging by damaging the DNA directly.^{3–5} Occupational exposure to high temperatures among soldiers, builders, and boiler workers is associated with considerable skin damage. Long-term skin exposure to direct heat leads to reticular pigmentation and telangiectasia formation, also known as erythema ab igne (EAI).⁶ However, so far, only a little is known about the actual effect of heat exposure on skin pigmentation and its underlying mechanism.

The Hedgehog (Hh) signaling pathway is an evolutionarily conserved pathway that plays a significant role in the normal embryonic development of invertebrates and vertebrates.⁷ Studies show that external stimuli like ultraviolet radiation b (UVB) exposure can activate the Hh signaling pathway⁸ and its key regulatory molecules including patched 1 (PTCH1), patched 2 (PTCH2), and Glioma-associated oncogene homologue 1 (GLI1).⁹ The upregulation of these genes is indicative of Hh pathway activation. The target genes of this pathway include vascular endothelial growth factor A (VEGFA),¹⁰ B-cell lymphoma 2 (BCL2),¹¹ BHLH transcription factor (MYCN),¹² members of the Wnt signaling pathway,¹³ etc.

The epidermal melanin unit (EMU) plays an important role in skin pigmentation.¹⁴ Melanocytes synthesize melanin, and so formed melanin gets transferred to the neighboring keratinocytes to protect the skin from ultraviolet (UV) damage.¹⁵ At the same time, keratinocytes affect melanin production by secreting paracrine factors in response to external stimuli, such as UV irradiation, inflammation, or drugs.¹⁶ Recent studies have suggested that paracrine factors, such as prostaglandin-endoperoxide synthase 2 (PTGS2) and vascular endothelial growth factor (VEGF), regulate melanin synthesis.^{17,18} The Wnt signaling pathway also plays an important role in melanogenesis and melanocyte development.^{19,20} The pathway is activated once the Wnt protein binds to its receptor, and it has crucial ligands named WNT3 and WNT7A.²¹

¹Department of Dermatology, The Third Xiangya Hospital, Central South University, Changsha, Hunan 410013, P.R. China

²Center of Medical Laboratory Animal, Hunan Academy of Chinese Medicine, Changsha, Hunan 410013, P.R. China

³Lead contact

*Correspondence:

zengqinghai@csu.edu.cn

<https://doi.org/10.1016/j.isci.2023.106749>



The exact pathogenesis of skin hyperpigmentation is unclear, although excessive UV radiation, exposure to particulate matter (PM) 2.5, and drugs have been implicated.^{22–25} By now, few studies have reported the effect of heat exposure on melanogenesis.²⁶ In this study, we investigated the effects of heat exposure on skin pigmentation using *in vitro* and *in vivo* models and found that heat promotes melanogenesis by increasing the paracrine effects in keratinocytes via the transient receptor potential vanilloid (TRPV) 3/Ca²⁺/Hh signaling pathway.

RESULTS

Heat exposure increased epidermal pigmentation in human skin

EAI is primarily induced by heat and manifests as local telangiectasia reticular erythema and pigmentation. Hematoxylin and eosin (H&E) staining and Fontana-Masson staining of human skin specimens confirmed the presence of more melanin particles in the basal layer of EAI skin than in normal skin (Figures 1A and 1B). To further establish the effects of heat on skin pigmentation, human skin tissues were exposed to heat for 5 days and stained as above. As shown in Figures 1C and 1D, heat exposure significantly increased the number of melanin granules.

Conditioned media from heat-treated HaCaT cells and keratinocytes promoted melanogenesis in pigment cells

The MNT1 and HaCaT cells were cultured at 37°C, 39°C, 41°C, 42°C, and 43°C for 24, 48, and 72 h, and the viability rates were evaluated by the Cell Counting Kit-8 (CCK-8) assay. As shown in Figures 2A and 2B, the viability of cells was unaffected at 37°C, 39°C, and 41°C. Therefore, we exposed the cells to these temperatures for 1 h daily over 3 consecutive days. Heat exposure significantly increased the melanin content (Figure 2C) as well as the expression of melanogenesis-related genes (Figure 2D) in the MNT1 cells, which was consistent with a previous report.²⁷ The MNT1 and HaCaT cells were then co-cultured in 1:10 ratio and exposed to heat for 3 days. As shown in Figures 2E and 2F, heat exposure increased the melanin content and the expression of melanogenesis-related genes in the co-cultured cells. Consistent with this, MNT1 cells cultured in the conditioned medium of heat-treated HaCaT cells also exhibited higher melanin content and expression levels of melanogenesis-related genes compared to the 37°C-control group (Figures 2G–2I), and the increased melanogenesis was associated with the activation of the mitogen-activated protein kinase (MAPK) and Wnt/ β -catenin pathways (Figures 2I and S1G). In addition, the conditioned medium of heat-exposed HaCaT cells also increased the number of Pmel17-expressing melanosomes along the dendrites of MNT1 cells (Figure 2J). On the other hand, we further validated our findings with primary cells. Human epidermal melanocytes (HEMs) cultured in the conditioned medium of heat-treated primary keratinocytes also exhibited higher melanin content (Figure S2A). Taken together, the conditioned medium of heat-treated HaCaT cells and keratinocytes significantly increased the melanin content and upregulated the melanogenesis-related genes of the pigment cells.

Heat-induced paracrine effects in HaCaT cells and keratinocytes were mediated via the Hh signaling pathway

To further explore the paracrine effects of heat on the HaCaT cells and keratinocytes, we exposed the cells to high temperatures for 3 days. We analyzed the changes in gene expression levels. Heat exposure significantly increased the expression of *VEGF*, *PTGS2*, *WNT3*, and *WNT7A* in HaCaT cells (Figure 3A) and keratinocytes (Figure S2B). The expression levels of other paracrine factors are shown in Figure S1A. Furthermore, high-throughput RNA sequencing revealed differentially expressed genes (DEGs) between the control and heat-treated cells (Figure 3B). The principal-component analysis (PCA) map of the genes is shown in Figure 3C. At the same time, gene set enrichment analysis (GSEA)-kyoto encyclopedia of genes and genomes (KEGG) revealed significant enrichment of the Hh, Wnt, and estrogen signaling pathways among others (Figure 3E). In addition, there was a significant positive correlation between heat exposure and the Hh, Wnt, estrogen, and GnRH signaling pathways (Figure 3F). Furthermore, we treated the HaCaT cells with the agonists of these signaling pathways (SAG-2.5 μ M, CT99021-5 μ M, DHEA-10 μ M, and Elagolix Sodium-10 μ M, respectively) for 24h and found that only the activation of the Hh signaling pathway significantly upregulated *VEGF*, *PTGS2*, *WNT3*, and *WNT7A* (Figure 3G). Inhibition of the Hh signaling pathway downregulated *VEGF*, *PTGS2*, *WNT3*, and *WNT7A* mRNA levels in HaCaT cells (Figure S1D). In contrast, the Hh pathway did not affect the fibroblast growth factor 2 (FGF2) levels (Figure S1B), indicating that other signaling pathways may activate it. The MNT1 cells were cultured in the conditioned medium of HaCaT cells supplemented with SAG (2.5 μ M). As shown in Figure 3H, the melanin levels were

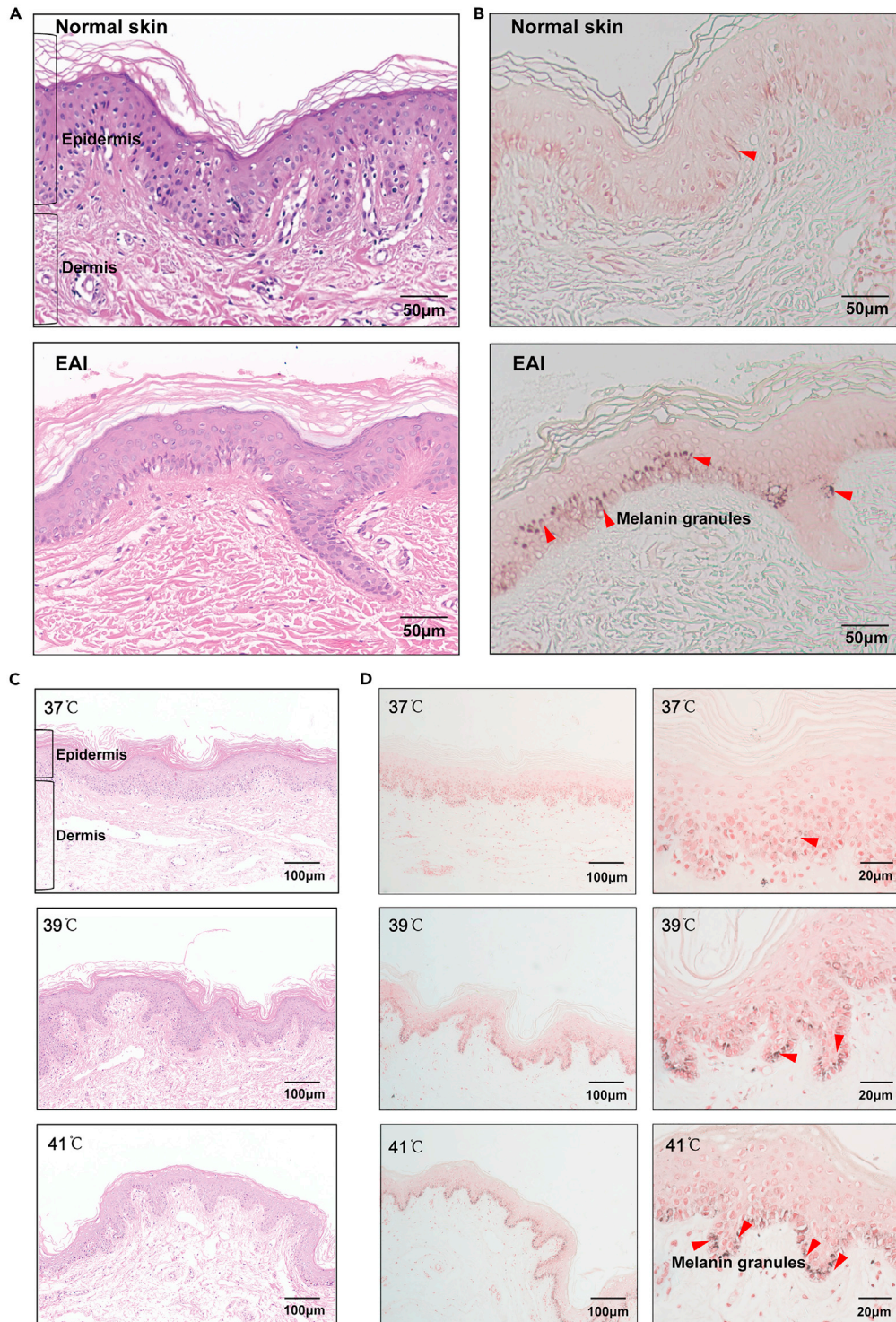


Figure 1. Heat promoted epidermal pigmentation in human skin tissue

Representative images of EAI and normal skin tissue sections stained with H&E (A) and Masson-Fontana dye (B). Scale bar = 50 μm . Representative images of heat-exposed human skin tissue from foreskins stained with H&E (C) and Masson-Fontana dye (D). Scale bar = 100 μm . As shown by the red arrows, the melanin granules were stained black or brown-black by the Masson-Fontana dye. The nucleus was stained blue, while cytoplasm, muscle fibers, collagen fibers, and red blood cells were stained in varying shades of red by H&E dyes in skin tissues. The images shown are representative from three independent biological experiments.

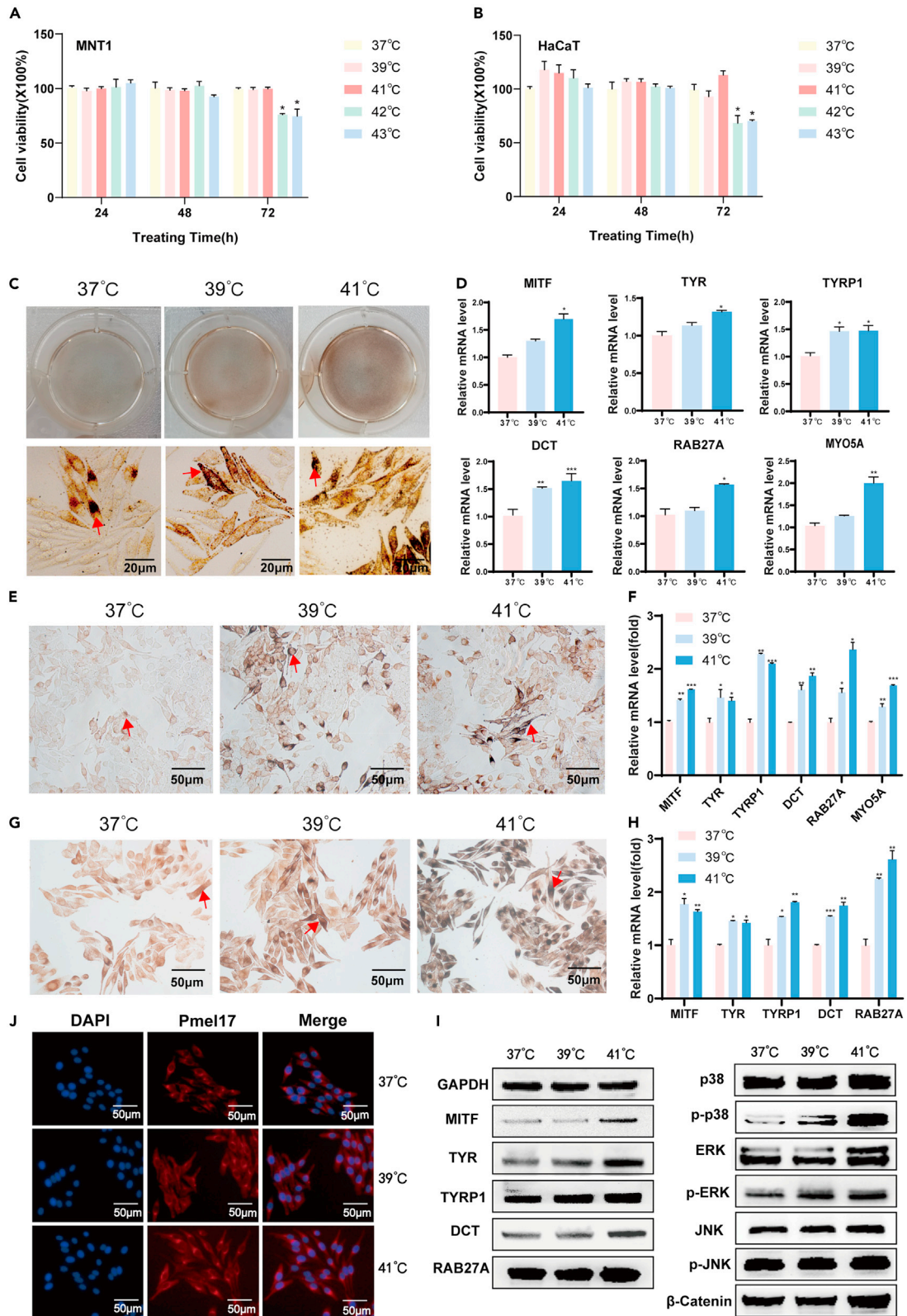


Figure 2. Conditioned media from heat-treated HaCaT cells promoted melanogenesis in MNT1 cells

Viability of MNT1 (A) and HaCaT (B) cells exposed to high temperatures for 24h, 48h, and 72h.
(C) Representative images of heat-exposed MNT1 cells stained with Masson-Fontana dye. Scale bar = 20 μm .
(D) Expression levels of melanogenesis-related genes in MNT1 cells exposed to heat.
(E) Representative images of heat-exposed and co-cultured MNT1 and HaCaT cells stained with Masson-Fontana dye. Scale bar = 50 μm .
(F) Expression levels of melanogenesis-related genes in the above cells.
(G) Representative images of MNT1 cells cultured in the conditioned medium of heat-exposed HaCaT cells and stained with Masson-Fontana dye. Scale bar = 50 μm .
(H) Expression levels of melanogenesis-related genes in the above cells.
(I) Immunoblot showing expression levels of melanogenesis-related, MAPK, and the Wnt signaling pathway proteins in the indicated cells.
(J) Representative immunofluorescence images showing melanosomes in the indicated cells. Scale bar = 50 μm . As shown by the red arrows, the melanin granules were stained black or brown-black by Masson-Fontana dye. Data are represented as mean \pm SD for n = 3 replicates. Statistical significance is shown as * for $p < 0.05$, ** for $p < 0.01$, and *** for $p < 0.001$, as evaluated by one-way ANOVA.

significantly higher in the treated versus the untreated MNT1 cells. In addition, PTCH1 and GLI1 were significantly upregulated in the HaCaT cells and keratinocytes after heat treatment (Figures 3I and S2D). It indicates that heat exposure regulates the Hh signaling pathway in keratinocytes.

Heat-induced TRPV3-mediated Ca^{2+} influx activated the Hh signaling pathway in HaCaT cells and keratinocytes

Transient receptor potential vanilloid (TRPV) plays a key role in relaying heat or pain sensations. Different TRPV channels have different sensitivity to temperature. Our study found that heat exposure upregulated TRPV3 level in HaCaT cells (Figure 4A) and keratinocytes (Figure S2C). We also tested the influence of heat on other TRPV channels such as TRPV1, 2, and 4. As shown in Figure S1F, the expression level of TRPV1, 2, and 4 did not significantly changed after heat exposure. Furthermore, activation of TRPV3 using its specific agonist (camphor, 50 μM) led to increased Ca^{2+} influx into the HaCaT cells (Figure 4B). Likewise, heat exposure also increased intracellular calcium levels in the HaCaT cells, and supplementation of TRPV3 inhibitors (TRPV3 antagonist 74a, 100 μM) was able to reverse the increased Ca^{2+} influx in response to heat (Figure 4C). We further explored the role of other TRPV channels in heat-induced calcium influx. TRPV1 agonists (vanilloid, 25 μM) or TRPV4 agonists (GSK1016790A, 50 nM) induce increased Ca^{2+} influx into HaCaT cells (Figure S3A). However, TRPV1 antagonists (AMG-517, 0.25 nM) or TRPV4 antagonists (GSK2193874, 50 nM) could not reverse the increased Ca^{2+} influx induced by heat exposure (Figure S3B). These suggested that TRPV1 and TRPV4 might not play critical roles in heat-induced calcium influx in cells. The conditioned medium of the camphor-treated HaCaT cells also increased the melanin content in MNT1 cells (Figure 4D). The proteins of the Hh signaling pathway were also upregulated in the camphor-treated HaCaT cells (Figure 4E). Furthermore, heat failed to activate the Hh pathway effectively after a TRPV3 inhibitor was used in HaCaT cells (Figure S1E). Inhibition of the Hh signaling pathway did not affect heat-induced upregulation of TRPV3, which suggested TRPV3 might be upstream of Hh signaling pathway (Figure S1C). Taken together, the TRPV3/ Ca^{2+} /Hh signaling pathway is most likely involved in heat-induced melanogenesis.

Heat exposure activated the Hh signaling pathway via TRPV3 in human skin tissue

To further determine the biological relevance of the Hh signaling pathway, we exposed human skin pieces to heat for 5 days and analyzed the *in situ* expression of the pathway proteins. As shown in Figure S4, PTCH1 and GLI1 were both highly expressed in the heat-treated human skin. TRPV3 agonists and inhibitors were added to test whether heat activated the Hh pathway in human skin tissue through TRPV3. Human skin pieces were exposed to heat for 5 days after the addition of TRPV3 agonists (camphor, 50 μM) or inhibitors (TRPV3 antagonist 74a, 100 μM). We found that the TRPV3 agonists increased heat-induced pigmentation and the TRPV3 inhibitors decreased it (Figure 5A). Furthermore, the expressions of PTCH1 and GLI1 were higher after treatment of TRPV3 agonists, while those were lower after treatment of TRPV3 inhibitors (Figure 5B). The above results indicated that heat activated the Hh signaling pathway via TRPV3.

DISCUSSION

This study shows that heat exposure induces paracrine effects in keratinocytes through the TRPV3/ Ca^{2+} /Hh signaling pathway, which promotes melanogenesis in melanocytes (Figure 6).

Previous studies have shown that the biological effects of heat and UVB on melanocytes are similar.²⁷ Furthermore, heat exposure can even augment UVB-induced tyrosinase activation and melanogenesis.²⁶ However, the specific mechanism underlying heat-induced melanogenesis has yet to be entirely understood. We found that

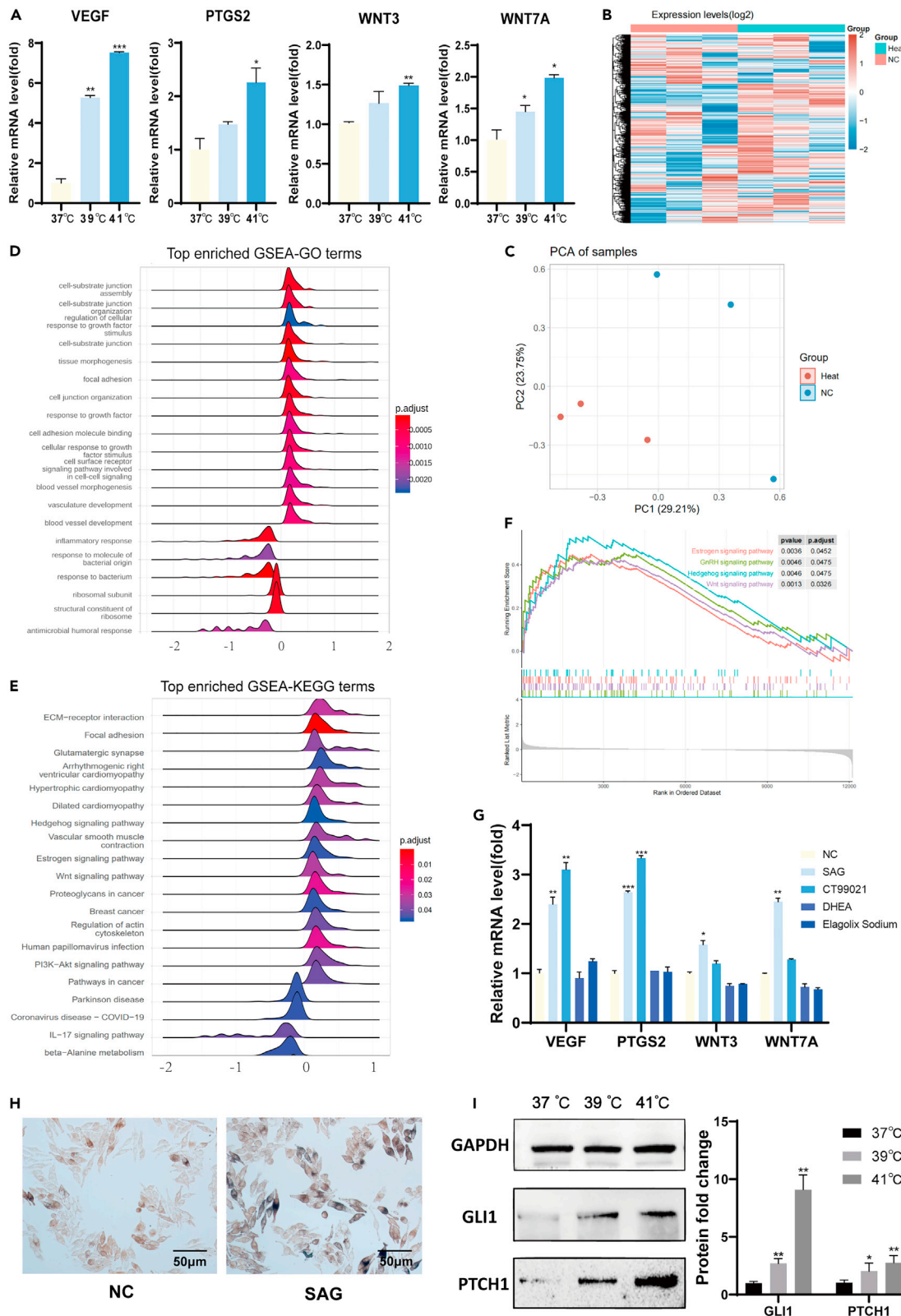


Figure 3. Heat-induced paracrine effects in HaCaT cells via the Hh signaling pathway

(A) *VEGF*, *PTGS2*, *WNT3*, and *WNT7A* mRNA levels in the indicated cells.

(B) The heatmap of the differentially expressed genes (DEGs).

(C) The Principal-Component Analysis (PCA) map.

(D) GO and (E) KEGG functional enrichment analysis.

(F) Gene Set Enrichment Analysis (GSEA) of the DEGs.

(G) *VEGF*, *PTGS2*, *WNT3*, and *WNT7A* mRNA levels in HaCaT cells treated with the indicated agonists.

(H) Representative images of MNT1 cells cultured in the conditioned medium of agonist-treated HaCaT cells and stained with Masson-Fontana dye.

(I) Immunoblot showing expression levels of Hh pathway proteins in the heat-exposed HaCaT cells. Scale bar = 50 μ m. Data are represented as mean \pm SD for n = 3 replicates. Statistical significance is shown as * for p < 0.05, ** for p < 0.01, and *** for p < 0.001, as evaluated by one-way ANOVA.

heat directly affects melanogenesis, which is consistent with previous studies.²⁷ The melanocytes and keratinocytes in the epidermis share a complex relationship. Keratinocytes secrete multiple paracrine factors that affect melanin production. Therefore, we evaluated these paracrine factors' role in heat-induced melanogenesis and found that heat exposure increased the melanin content and the expression of melanogenesis-related genes in co-cultured MNT1 and HaCaT cells. Furthermore, the conditioned medium of the heat-treated HaCaT cells and keratinocytes showed a similar melanogenic effect on pigment cells. In this study, heat exposure significantly increased the expression of *VEGF*, *PTGS2*, *WNT3*, and *WNT7A* in HaCaT cells and keratinocytes. These paracrine factors have been reported to be involved in regulating melanin synthesis. VEGF interacts with VEGF receptors (VEGFRs) and promotes melanogenesis by activating MAPK signaling pathway.²⁸ *PTGS2* plays an important role in prostaglandin E2 (PGE2) production, which promotes melanogenesis by interacting with the EP receptor and activating the cyclic AMP (cAMP) signaling pathway in epidermal melanocytes.^{29,30} *WNT3* and *WNT7A* might act as ligands in activating the Wnt/ β -catenin pathways by binding to its receptors and promoting the expression of melanogenesis-related genes.³¹ Altogether, heat might promote melanogenesis by augmenting the paracrine effects of keratinocytes.

Nevertheless, the heat-induced paracrine effects of keratinocytes remain unclear. The Hh signaling pathway mediates thermal allodynia and hyperalgesia following skin damage due to UV irradiation.³² High-throughput RNA sequencing revealed a significant positive correlation between heat exposure and the Hh signaling pathway, indicating that heat can activate this pathway. Furthermore, activation of the Hh signaling pathway upregulated *VEGF*, *PTGS2*, *WNT3*, and *WNT7A* in the HaCaT cells. In addition, the conditioned medium of HaCaT cells treated with an Hh pathway agonist increased the melanin content of the MNT1 cells. These results suggest that heat-induced paracrine effects in keratinocytes are most likely mediated via the Hh signaling pathway.

Transient receptor potential (TRP) channels act as polymodal sensors that relay various chemical and physical stimuli and induce cellular and physiological responses.³³ TRPV3 is a member of the vanilloid subfamily or TRPV channels and is highly expressed in skin keratinocytes where it forms Ca²⁺-permeable non-selective cation channels to regulate various cutaneous functions.^{34–40} TRPV3 plays an important role in many cutaneous sensations, including nociception, thermal sensing, and itching.^{36,38} Keratinocytes also express other TRPV channels, such as TRPV1 and TRPV4.^{41–43} TRPV1, a heat-gated channel, was found in human keratinocytes recently. Furthermore, the activation of epidermal TRPV1 was known to induce the release of proinflammatory mediators.⁴⁴ TRPV4 channel is a physiological sensor for hypoosmolarity, mechanical deformation, and warm temperature.⁴⁵ TRPV1 is activated by noxious heat (>43°C), while TRPV3 is activated at the warm temperature threshold of 33°C and exhibits increasing responses at higher noxious temperatures. TRPV4, identified originally as an osmosensory ion channel, is also activated by warm temperatures (25–34°C). Although both TRPV3 and TRPV4 are expressed in keratinocytes and are activated by a similar range of temperatures, these channels likely have distinct functions in the skin.⁴⁶ Our study found that heat-induced TRPV3 can effectively induce Ca²⁺ influx and activate the Hh signaling pathway. The expression level of TRPV1 and 4 did not significantly change after heat exposure (39–41°C), and TRPV1 antagonists or TRPV4 antagonists could not reverse the increased Ca²⁺ influx induced by heat exposure (39–41°C). These results suggest that TRPV3 rather than TRPV1 or 4 may play a key role in heat-induced (39–41°C) calcium influx in keratinocytes. Furthermore, the conditioned medium of HaCaT cells treated with the TRPV3 agonist increased the melanin content in MNT1 cells. Thus, heat-induced TRPV3 may play a role in melanogenesis by activating the Hh signaling pathway.

Long-term or repeated exposure of skin to heat deepens erythema, resulting in reticular telangiectasia, skin atrophy, pigmentation, and diffuse hyperkeratosis, which are characteristic of EAI and similar to skin

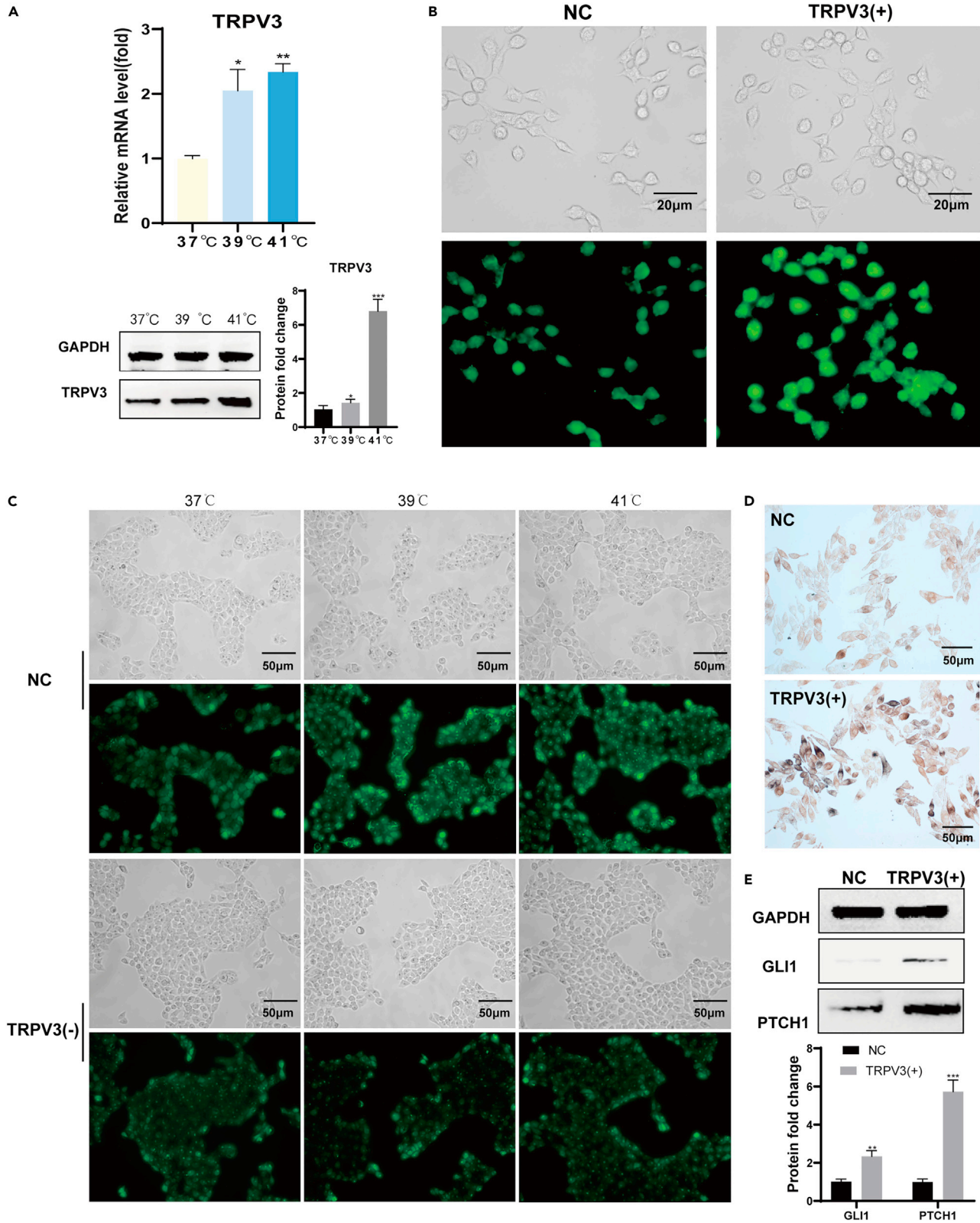


Figure 4. Heat-induced TRPV3-mediated Ca²⁺ influx activated the Hh signaling pathway in HaCaT cells

(A) mRNA and protein levels of TRPV3 in heat-exposed HaCaT cells.
(B) Representative images of HaCaT cells stained with Fluo-4-AM solution showing intracellular calcium. Scale bar = 20 μm.
(C) Representative images of HaCaT cells stained with Fluo-4-AM solution showing intracellular calcium. Scale bar = 50 μm.
(D) Representative images of MNT1 cells cultured in the conditioned medium of camphor-treated HaCaT cells and stained with Masson-Fontana dye.
(E) Immunoblot showing expression levels of Hh pathway proteins in the camphor-treated HaCaT cells. Data are represented as mean ± SD for n = 3 replicates. Statistical significance is shown as * for p < 0.05, ** for p < 0.01, and *** for p < 0.001, as evaluated by one-way ANOVA and unpaired t-test.

heterochromism.⁴⁷ However, the exact pathological basis of EAI remains unclear. Our findings show that heat promotes melanogenesis, which may explain the pigmentation in EAI skin lesions. In addition, heat exposure also increased the expression of VEGF, a growth factor involved in normal and pathological angiogenesis, in the HaCaT cells.⁴⁸ Therefore, heat-induced VEGF may alter the development of blood vessels in EAI. Overall, heat exposure (39–41°C) triggers melanogenesis by increasing the paracrine effects in keratinocytes via the TRPV3/Ca²⁺/Hh signaling pathway. Our study provides insights into the mechanisms of heat-induced skin diseases such as EAI and hints toward pathways that could be therapeutic targets.

Limitations of the study

The effect of heat on melanogenesis has yet to be verified in animal models, and experiments on cell culture and skin explants might differ from the actual physiological state. It would be more convincing to test whether Hh signaling is activated by heat in TRPV3 knockout mice. In addition, the effectors involved in the Hh signaling pathway during heat-induced melanogenesis need further investigation, and further experiments are required.

STAR★METHODS

Detailed methods are provided in the online version of this paper and include the following:

- KEY RESOURCES TABLE
- RESOURCE AVAILABILITY
 - Lead contact
 - Materials availability
 - Data and code availability
- EXPERIMENTAL MODEL AND SUBJECT DETAILS
 - Cell lines
- METHOD DETAILS
 - Cell viability assay
 - Masson-Fontana melanin staining
 - Western blotting
 - Immunofluorescence
 - Quantitative reverse transcription-polymerase chain reaction (qRT-PCR)
 - Human skin samples
 - Immunohistochemistry
 - Cytoplasmic Ca²⁺ measurement
 - RNA high-throughput sequencing
- QUANTIFICATION AND STATISTICAL ANALYSIS

SUPPLEMENTAL INFORMATION

Supplemental information can be found online at <https://doi.org/10.1016/j.isci.2023.106749>.

ACKNOWLEDGMENTS

This study was supported by financial grants from the National Natural Science Foundation of China (82073420), the Natural Science Foundation of Hunan Province (2021JJ20089), the Wisdom Accumulation and Talent Cultivation Project of the Third Xiangya Hospital of Central South University (YX202007), and the Science and Technology Innovation Program of Hunan Province (2021RC3035).

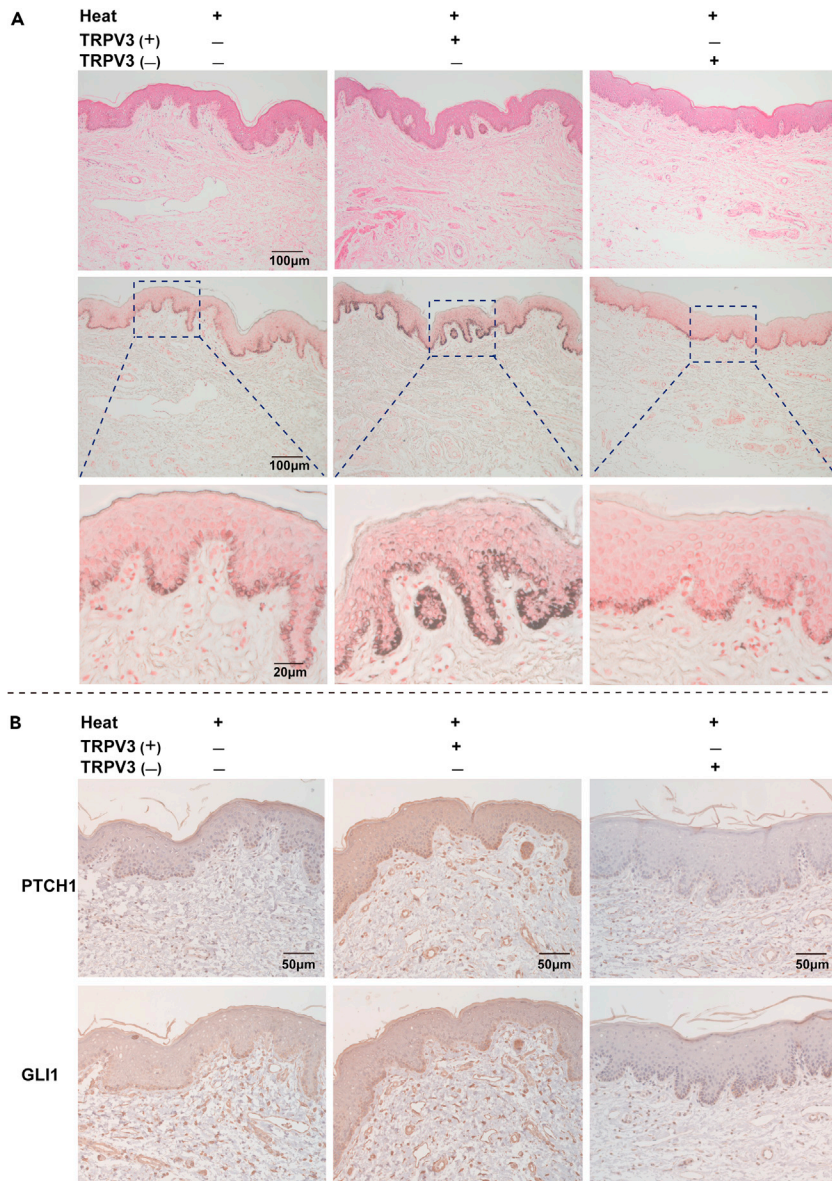


Figure 5. Heat exposure activated the Hh signaling pathway via TRPV3 in human skin tissue

The foreskin tissue of the same volunteer was randomly divided into 9 skin pieces with same size and color. These skin pieces were randomly divided into three groups; each group was treated with heat, heat+TRPV3 agonists, and heat+TRPV3 inhibitors, respectively.

(A) Representative images of human skin tissues stained with H&E and Masson-Fontana dye. Scale bar = 100 μ m.

(B) Representative images of human skin tissues showing *in situ* expression of PTCH1 and GLI1. Scale bar = 50 μ m. The images shown are representative from three independent biological experiments.

AUTHOR CONTRIBUTIONS

Conceived and designed the experiments and analyzed data: Q.Z., J.C., J.H., and H.Z.; Performed most of the experiments: L.Z., Y.Z., X.Z., and F.Z.; Performed bioinformatics analysis: C.F., L.J., Y.H., and L.Z.; Wrote the manuscript: L.Z.; All authors contributed to and approved the paper.

DECLARATION OF INTERESTS

The authors declare that they have no competing interests.

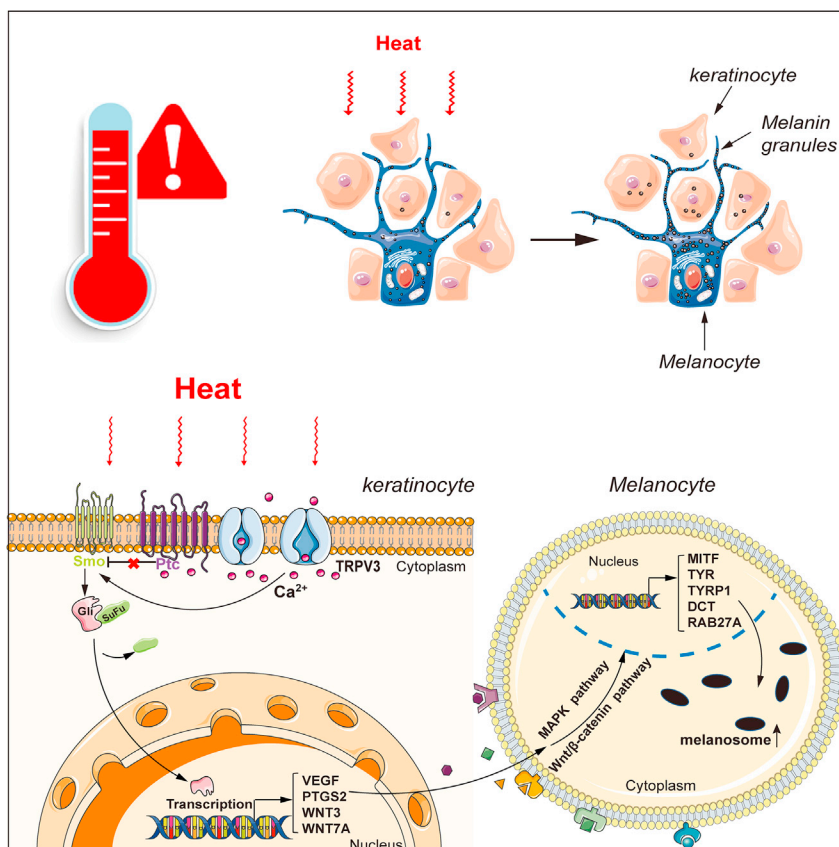


Figure 6. Schematic presentation of the mechanism underlying heat-induced melanogenesis

INCLUSION AND DIVERSITY

We support inclusive, diverse, and equitable conduct of research. We worked to ensure diversity in experimental samples through the selection of the cell lines.

Received: September 3, 2022

Revised: March 10, 2023

Accepted: April 21, 2023

Published: April 26, 2023

REFERENCES

- Yardman-Frank, J.M., and Fisher, D.E. (2021). Skin pigmentation and its control: from ultraviolet radiation to stem cells. *Exp. Dermatol.* 30, 560–571. <https://doi.org/10.1111/exd.14260>.
- The, L. (2018). Heatwaves and health. *Lancet* 392, 359. [https://doi.org/10.1016/S0140-6736\(18\)30434-3](https://doi.org/10.1016/S0140-6736(18)30434-3).
- Dewey, W.C., Hopwood, L.E., Sapareto, S.A., and Gerweck, L.E. (1977). Cellular responses to combinations of hyperthermia and radiation. *Radiology* 123, 463–474. <https://doi.org/10.1148/123.2.463>.
- Schieke, S.M., Schroeder, P., and Krutmann, J. (2003). Cutaneous effects of infrared radiation: from clinical observations to molecular response mechanisms. *Photodermatol. Photoimmunol. Photomed.* 19, 228–234. <https://doi.org/10.1034/j.1600-0781.2003.00054.x>.
- Schroeder, P., Haendeler, J., and Krutmann, J. (2008). The role of near infrared radiation in photoaging of the skin. *Exp. Gerontol.* 43, 629–632. <https://doi.org/10.1016/j.exger.2008.04.010>.
- Knöpfel, N., and Weibel, L. (2021). Erythema Ab Igne. *JAMA Dermatol.* 157, 106. <https://doi.org/10.1001/jamadermatol.2020.3995>.
- Varjosalo, M., and Taipale, J. (2008). Hedgehog: functions and mechanisms. *Genes Dev.* 22, 2454–2472. <https://doi.org/10.1101/gad.1693608>.
- Kim, W., Kim, E., Yang, H.J., Kwon, T., Han, S., Lee, S., Youn, H., Jung, Y., Kang, C., and Youn, B. (2015). Inhibition of hedgehog signalling attenuates UVB-induced skin photoaging. *Exp. Dermatol.* 24, 611–617. <https://doi.org/10.1111/exd.12735>.
- Bonifas, J.M., Pennypacker, S., Chuang, P.T., McMahon, A.P., Williams, M., Rosenthal, A., De Sauvage, F.J., and Epstein, E.H., Jr. (2001). Activation of expression of hedgehog target genes in basal cell carcinomas. *J. Invest. Dermatol.* 116, 739–742. <https://doi.org/10.1046/j.1523-1747.2001.01315.x>.
- Morrow, D., Cullen, J.P., Liu, W., Guha, S., Sweeney, C., Birney, Y.A., Collins, N., Walls, D., Redmond, E.M., and Cahill, P.A. (2009). Sonic Hedgehog induces Notch target gene

- expression in vascular smooth muscle cells via VEGF-A. *Arterioscler. Thromb. Vasc. Biol.* 29, 1112–1118. <https://doi.org/10.1161/ATVBAHA.109.186890>.
11. Bigelow, R.L.H., Chari, N.S., Unden, A.B., Spurgers, K.B., Lee, S., Roop, D.R., Toftgard, R., and McDonnell, T.J. (2004). Transcriptional regulation of bcl-2 mediated by the sonic hedgehog signaling pathway through gli-1. *J. Biol. Chem.* 279, 1197–1205. <https://doi.org/10.1074/jbc.M310589200>.
 12. Oliver, T.G., Grasfeder, L.L., Carroll, A.L., Kaiser, C., Gillingham, C.L., Lin, S.M., Wickramasinghe, R., Scott, M.P., and Wechsler-Reya, R.J. (2003). Transcriptional profiling of the Sonic hedgehog response: a critical role for N-myc in proliferation of neuronal precursors. *Proc. Natl. Acad. Sci. USA* 100, 7331–7336. <https://doi.org/10.1073/pnas.0832317100>.
 13. Katoh, M., and Katoh, M. (2006). Notch ligand, JAG1, is evolutionarily conserved target of canonical WNT signaling pathway in progenitor cells. *Int. J. Mol. Med.* 17, 681–685.
 14. Nordlund, J.J. (2007). The melanocyte and the epidermal melanin unit: an expanded concept. *Dermatol. Clin.* 25, 271–281. <https://doi.org/10.1016/j.det.2007.04.001>.
 15. Boissy, R.E. (2003). Melanosome transfer to and translocation in the keratinocyte. *Exp. Dermatol.* 12 (Suppl 2), 5–12. <https://doi.org/10.1034/j.1600-0625.12.s2.1.x>.
 16. Wang, Y., Viennet, C., Robin, S., Berthon, J.Y., He, L., and Humbert, P. (2017). Precise role of dermal fibroblasts on melanocyte pigmentation. *J. Dermatol. Sci.* 88, 159–166. <https://doi.org/10.1016/j.jdermsci.2017.06.018>.
 17. Yuan, X.H., and Jin, Z.H. (2018). Paracrine regulation of melanogenesis. *Br. J. Dermatol.* 178, 632–639. <https://doi.org/10.1111/bjcd.15651>.
 18. Kim, J.Y., Shin, J.Y., Kim, M.R., Hann, S.K., and Oh, S.H. (2012). siRNA-mediated knock-down of COX-2 in melanocytes suppresses melanogenesis. *Exp. Dermatol.* 21, 420–425. <https://doi.org/10.1111/j.1600-0625.2012.01483.x>.
 19. Zhu, J.W., Ni, Y.J., Tong, X.Y., Guo, X., and Wu, X.P. (2020). Activation of VEGF receptors in response to UVB promotes cell proliferation and melanogenesis of normal human melanocytes. *Exp. Cell Res.* 387, 111798. <https://doi.org/10.1016/j.yexcr.2019.111798>.
 20. O'Connell, M.P., and Weeraratna, A.T. (2009). Hear the Wnt Ror: how melanoma cells adjust to changes in Wnt. *Pigment Cell Melanoma Res.* 22, 724–739. <https://doi.org/10.1111/j.1755-148X.2009.00627.x>.
 21. Zhan, Z., Zhang, X., Huang, J., Huang, Y., Huang, Z., Pan, X., Quan, G., Liu, H., Wang, L., and Wu, A.C. (2017). Improved gene transfer with functionalized hollow mesoporous silica nanoparticles of reduced cytotoxicity. *Materials* 10, 731. <https://doi.org/10.3390/ma10070731>.
 22. Nie, X., Liu, H., Liu, L., Wang, Y.D., and Chen, W.D. (2020). Emerging roles of Wnt ligands in human colorectal cancer. *Front. Oncol.* 10, 1341. <https://doi.org/10.3389/fonc.2020.01341>.
 23. Costin, G.E., and Hearing, V.J. (2007). Human skin pigmentation: melanocytes modulate skin color in response to stress. *FASEB J* 21, 976–994. <https://doi.org/10.1096/fj.06-6649rev>.
 24. Yamaguchi, Y., and Hearing, V.J. (2009). Physiological factors that regulate skin pigmentation. *Biofactors* 35, 193–199. <https://doi.org/10.1002/biof.29>.
 25. Shi, Y., Zeng, Z., Liu, J., Pi, Z., Zou, P., Deng, Q., Ma, X., Qiao, F., Xiong, W., Zhou, C., et al. (2021). Particulate matter promotes hyperpigmentation via AhR/MAPK signaling activation and by increasing alpha-MSH paracrine levels in keratinocytes. *Environ. Pollut.* 278, 116850. <https://doi.org/10.1016/j.envpol.2021.116850>.
 26. Gu, W.J., Ma, H.J., Zhao, G., Yuan, X.Y., Zhang, P., Liu, W., Ma, L.J., and Lei, X.B. (2014). Additive effect of heat on the UVB-induced tyrosinase activation and melanogenesis via ERK/p38/MITF pathway in human epidermal melanocytes. *Arch. Dermatol. Res.* 306, 583–590. <https://doi.org/10.1007/s00403-014-1461-y>.
 27. Nakazawa, K., Sahuc, F., Damour, O., Collombel, C., and Nakazawa, H. (1998). Regulatory effects of heat on normal human melanocyte growth and melanogenesis: comparative study with UVB. *J. Invest. Dermatol.* 110, 972–977. <https://doi.org/10.1046/j.1523-1747.1998.00204.x>.
 28. Zhu, J.W., Ni, Y.J., Tong, X.Y., Guo, X., Wu, X.P., and Lu, Z.F. (2020). Tranexamic acid inhibits angiogenesis and melanogenesis in vitro by targeting VEGF receptors. *Int. J. Med. Sci.* 17, 903–911. <https://doi.org/10.7150/ijms.44188>.
 29. Li, M., Gao, Y., Li, C., Liu, L., Li, K., Gao, L., Wang, G., Zhang, Z., and Gao, T. (2009). Association of COX2 functional polymorphisms and the risk of vitiligo in Chinese populations. *J. Dermatol. Sci.* 53, 176–181. <https://doi.org/10.1016/j.jdermsci.2008.09.010>.
 30. Starner, R.J., McClelland, L., Abdel-Malek, Z., Fricke, A., and Scott, G. (2010). PGE(2) is a UVR-inducible autocrine factor for human melanocytes that stimulates tyrosinase activation. *Exp. Dermatol.* 19, 682–684. <https://doi.org/10.1111/j.1600-0625.2010.01074.x>.
 31. Guo, H., Yang, K., Deng, F., Ye, J., Xing, Y., Li, Y., Lian, X., and Yang, T. (2012). Wnt3a promotes melanin synthesis of mouse hair follicle melanocytes. *Biochem. Biophys. Res. Commun.* 420, 799–804. <https://doi.org/10.1016/j.bbrc.2012.03.077>.
 32. Babcock, D.T., Shi, S., Jo, J., Shaw, M., Gutstein, H.B., and Galko, M.J. (2011). Hedgehog signaling regulates nociceptive sensitization. *Curr. Biol.* 21, 1525–1533. <https://doi.org/10.1016/j.cub.2011.08.020>.
 33. Moore, C., and Liedtke, W.B. (2017). Osmomechanical-sensitive TRPV channels in mammals. In *Neurobiology of TRP Channels*, T.L.R. Emir, ed., pp. 85–94. <https://doi.org/10.4324/9781315152837-5>.
 34. Yang, P., and Zhu, M.X. (2014). TRPV3. *Handb. Exp. Pharmacol.* 222, 273–291. https://doi.org/10.1007/978-3-642-54215-2_11.
 35. Luo, J., and Hu, H. (2014). Thermally activated TRPV3 channels. *Curr. Top. Membr.* 74, 325–364. <https://doi.org/10.1016/B978-0-12-800181-3.00012-9>.
 36. Wang, Y., Li, H., Xue, C., Chen, H., Xue, Y., Zhao, F., Zhu, M.X., and Cao, Z. (2021). TRPV3 enhances skin keratinocyte proliferation through EGFR-dependent signaling pathways. *Cell Biol. Toxicol.* 37, 313–330. <https://doi.org/10.1007/s10565-020-09536-2>.
 37. Szöllösi, A.G., Vasas, N., Angyal, Á., Kistamás, K., Nánási, P.P., Mihály, J., Béke, G., Herczeg-Liszes, E., Szegedi, A., Kawada, N., et al. (2018). Activation of TRPV3 regulates inflammatory actions of human epidermal keratinocytes. *J. Invest. Dermatol.* 138, 365–374. <https://doi.org/10.1016/j.jid.2017.07.852>.
 38. Zhao, J., Munanairi, A., Liu, X.Y., Zhang, J., Hu, L., Hu, M., Bu, D., Liu, L., Xie, Z., Kim, B.S., et al. (2020). PAR2 mediates itch via TRPV3 signaling in keratinocytes. *J. Invest. Dermatol.* 140, 1524–1532. <https://doi.org/10.1016/j.jid.2020.01.012>.
 39. Vasas, N., Pénez, Z., Kistamás, K., Nánási, P.P., Molnár, S., Szegedi, A., Szöllösi, A.G., and Bíró, T. (2022). Transient receptor potential vanilloid 3 expression is increased in non-lesional skin of atopic dermatitis patients. *Exp. Dermatol.* 31, 807–813. <https://doi.org/10.1111/exd.14530>.
 40. Park, C.W., Kim, H.J., Choi, Y.W., Chung, B.Y., Woo, S.Y., Song, D.K., and Kim, H.O. (2017). TRPV3 channel in keratinocytes in scars with post-burn pruritus. *Int. J. Mol. Sci.* 18, 2425. <https://doi.org/10.3390/ijms18112425>.
 41. Tóth, B.I., Dobrosi, N., Dajnoki, A., Czifra, G., Oláh, A., Szöllösi, A.G., Juhász, I., Sugawara, K., Paus, R., and Bíró, T. (2011). Endocannabinoids modulate human epidermal keratinocyte proliferation and survival via the sequential engagement of cannabinoid receptor-1 and transient receptor potential vanilloid-1. *J. Invest. Dermatol.* 131, 1095–1104. <https://doi.org/10.1038/jid.2010.421>.
 42. Ständer, S., Moormann, C., Schumacher, M., Buddenkotte, J., Artuc, M., Shpacovitch, V., Brzoska, T., Lippert, U., Henz, B.M., Luger, T.A., et al. (2004). Expression of vanilloid receptor subtype 1 in cutaneous sensory nerve fibers, mast cells, and epithelial cells of appendage structures. *Exp. Dermatol.* 13, 129–139. <https://doi.org/10.1111/j.0906-6705.2004.0178.x>.
 43. Kida, N., Sokabe, T., Kashio, M., Haruna, K., Mizuno, Y., Suga, Y., Nishikawa, K.,

- Kanamaru, A., Hongo, M., Oba, A., and Tominaga, M. (2012). Importance of transient receptor potential vanilloid 4 (TRPV4) in epidermal barrier function in human skin keratinocytes. *Pflugers Arch.* 463, 715–725. <https://doi.org/10.1007/s00424-012-1081-3>.
44. Li, W.H., Lee, Y.M., Kim, J.Y., Kang, S., Kim, S., Kim, K.H., Park, C.H., and Chung, J.H. (2007). Transient receptor potential vanilloid-1 mediates heat-shock-induced matrix metalloproteinase-1 expression in human epidermal keratinocytes. *J. Invest. Dermatol.* 127, 2328–2335. <https://doi.org/10.1038/sj.jid.5700880>.
45. Sokabe, T., Fukumi-Tominaga, T., Yonemura, S., Mizuno, A., and Tominaga, M. (2010). The TRPV4 channel contributes to intercellular junction formation in keratinocytes. *J. Biol. Chem.* 285, 18749–18758. <https://doi.org/10.1074/jbc.M110.103606>.
46. Dhaka, A., Viswanath, V., and Patapoutian, A. (2006). Trp ion channels and temperature sensation. *Annu. Rev. Neurosci.* 29, 135–161. <https://doi.org/10.1146/annurev.neuro.29.051605.112958>.
47. Kettelhut, E.A., Traylor, J., and Roach, J.P. (2022). *Erythema Ab Igne* (StatPearls).
48. Melincovici, C.S., Boşca, A.B., Şuşman, S., Mărginean, M., Mişu, C., Istrate, M., Moldovan, I.M., Roman, A.L., and Mişu, C.M. (2018). Vascular endothelial growth factor (VEGF) - key factor in normal and pathological angiogenesis. *Rom. J. Morphol. Embryol.* 59, 455–467.

STAR★METHODS

KEY RESOURCES TABLE

REAGENT or RESOURCE	SOURCE	IDENTIFIER
Antibodies		
Rabbit monoclonal anti-TYR	ZENBIO	Cat#121392; SwissProtID:P14679
Rabbit monoclonal anti-MITF	ZENBIO	Cat#R24980; SwissProtID:O75030
Rabbit monoclonal anti-TYRP1	ZENBIO	Cat#382326; SwissProtID:P17643
Rabbit monoclonal anti-DCT	ZENBIO	Cat#821374; SwissProtID:P40126
Rabbit monoclonal anti-RAB27A	Cell Signaling Technology	Cat#95394S; RRID: AB_2800247
Rabbit monoclonal anti-ERK	Cell Signaling Technology	Cat#4695S; RRID: AB_390779
Rabbit monoclonal anti- p-ERK	Cell Signaling Technology	Cat#4370S; RRID: AB_2315112
Rabbit monoclonal anti-JUK	Cell Signaling Technology	Cat#9252S; RRID: AB_2250373
Rabbit monoclonal anti-p-JUK	Cell Signaling Technology	Cat#9255S; RRID: AB_2307321
Rabbit monoclonal anti-p38	Cell Signaling Technology	Cat#8690S; RRID: AB_10999090
Rabbit monoclonal anti-p-p38	Cell Signaling Technology	Cat#4511S; RRID: AB_2139682
Rabbit monoclonal anti-β-catenin	ZENBIO	Cat#R22820; SwissProt ID: P35222
Rabbit monoclonal anti-GLI1	ABclonal	Cat#A14675; RRID: AB_2761550
Rabbit monoclonal anti-PTCH1	ABclonal	Cat#A0826; RRID: AB_2757415
Rabbit monoclonal anti-GAPDH	Cell Signaling Technology	Cat#5174S; RRID: AB_10622025
Mouse monoclonal anti-Pmel17	Santa Cruz Biotechnology	Cat#sc-377325; RRID: AB_2889982
Goat Anti-mouse IgG(H+L) Fluor 594	Affinity	Cat#S0005; RRID: AB_2843435
Chemicals, peptides, and recombinant proteins		
CT99021	Selleck	S1263; CAS:252917-06-9
Elagolix Sodium	Selleck	S4896; CAS:832720-36-2
Smoothened Agonist (SAG) HCl	Selleck	S7779; CAS:2095432-58-7
Dehydroepiandrosterone(DHEA)	Selleck	S5508; CAS:853-23-6
Vismodegib	Selleck	S1082; CAS:879085-55-9
TRPV3 antagonist 74a	MedChemExpress	HY-131868; CAS:1432051-63-2
Camphor	Selleck	S3851; CAS: 76-22-2
GSK1016790A	Selleck	S8107; CAS:942206-85-1
GSK2193874	Selleck	S8367; CAS:1336960-13-4
AMG-517	Selleck	S7115; CAS:659730-32-2
Capsaicin(Vanilloid)	Selleck	S1990; CAS:404-86-4
Deposited data		
RNA-seq	This paper	GEO accession numbers: GSE229915 (https://www.ncbi.nlm.nih.gov/geo/query/acc.cgi?acc=GSE229915)
Critical commercial assays		
Masson-Fontana	G-CLONE	400-910-1997; Cat.No.RS8020
qPCR SYBR Green Master Mix	YEASEN	LOT:H8210010; Cat:11184ES08
HiScript II Q RT SuperMix for qPCR	Vazyme	R223-01
Fluo-4 AM	Beyotime	S1060

(Continued on next page)

Continued

REAGENT or RESOURCE	SOURCE	IDENTIFIER
Experimental models: Cell lines		
MNT1	Meisen CTCC	CTCC-006-0301
HaCaT	Otwo Biotech (ShenZhen) Inc.	HTX2089
Melanocytes	N/A	N/A
Keratinocytes	N/A	N/A
Oligonucleotides		
See the Table S1	This paper	N/A
Software and algorithms		
Image J	Image J software	https://imagej.nih.gov/ij/
Adobe Illustrator 2021	N/A	https://www.adobe.com/products/illustrator.html
CaseViewer 2.4(64-bit version)	The Digital Pathology Company	https://www.3dhistech.com/solutions/caseviewer/
GraphPad Prism 9.0	GraphPad	https://www.graphpad.com/

RESOURCE AVAILABILITY**Lead contact**

Further information and requests for resources and reagents should be directed to and will be fulfilled by the lead contact, Qinghai Zeng (zengqinghai@csu.edu.cn).

Materials availability

This study did not generate new unique reagents.

Data and code availability

- RNA-seq data have been deposited at NCBI and are publicly available as of the date of publication. Accession numbers are listed in the [key resources table](#).
- This paper does not report original code.
- Any additional information required to reanalyze the data reported in this paper is available from the [lead contact](#) upon request.

EXPERIMENTAL MODEL AND SUBJECT DETAILS**Cell lines**

The human melanoma cell line MNT1 cells were obtained and authenticated from the Meisen CTCC (Zhejiang Meisen Cell Technology Co., LTD). Human immortalized keratinocyte line HaCaT cells were obtained and authenticated from Otwo Biotech (ShenZhen) Inc. MNT1 and HaCaT cells were cultured in DMEM (#C11995500BT, Gibco, NY) supplemented with 20% or 10% fetal bovine serum (FBS) and 1% penicillin-streptomycin (#ABT920, G-CLONE). Primary human epidermal melanocytes (HEMs) and keratinocytes were separated from male volunteers' foreskin (approved by donors and the Ethics Committee of the Third Xiangya Hospital, Central South University, Changsha, China). HEMs were cultured in 254 medium (M254500, Gibco) with 1% HMGS (M254500, Gibco) and 5% FBS, and keratinocytes were cultured in serum-free KGM. None of the cell lines were detected to be contaminated with mycoplasma. All cells were cultured in a humidified incubator at 37°C and 5% CO₂.

METHOD DETAILS**Cell viability assay**

Cell viability was tested by the Cell Counting Kit-8 (CCK-8) and was done according to the manufacturer's instructions (#BS350A, Biosharp). Briefly, the cells were seeded in 96-well plates at the density of 2000 cells/well, or 5000 cells/well, and incubated at different temperatures in a temperature-regulated incubator

(#HN-25BS, LICHEN). After 24h, 48h, and 72h of culture, 10 μ L CCK-8 reagent was added to each well, and the cells were incubated at 37°C for 1 hour. When the color of the medium turned orange, the reaction was terminated, and the absorbance was measured at 490 nm using a microplate reader (PerkinElmer EnVision Xcite, UK).

Masson-Fontana melanin staining

The adherent cultured cells were fixed with 4% paraformaldehyde for 15 min. After rinsing with water, the cells were stained with the Fontana ammonia-silver solution (#No.RS8020, G-GLONE) for 24 h in a dark chamber, rinsed again, and immersed in hyposulphite solution for 5 min. The slides were observed under an inverted microscope, and the melanin granules were counted.

Western blotting

The total cellular protein was extracted using RIPA Lysis Buffer (#No. EX6020, G-GLONE) supplemented with a protease inhibitor and phosphatase inhibitor cocktail (Roche) and quantified using a BCA protein assay kit (# KGPBCA, KeyGEN Biotec). After blocking with 1% BSA (#4240GR005, BioFroxx), the blots were incubated overnight with primary antibodies against *TYR* (#121392, ZENBIO), *MITF* (#R24980, ZENBIO), *TYRP1* (#382326, ZENBIO), *DCT* (#821374, ZENBIO), *RAB27A* (#95394S, CST), *ERK* (#4695S, CST), *p-ERK* (#4370S, CST), *JUK* (#9252S, CST), *p-JUK* (#9255S, CST), *p38* (#8690S, CST), *p-p38* (#4511S, CST), *β -catenin* (#R22820, ZENBIO), *GLI1* (#A14675, ABclonal), *PTCH1* (#A0826, ABclonal) and *GAPDH* (#5174S, CST) at 4°C. All antibodies were diluted to 1:1000, and the anti-GAPDH antibody was diluted to 1:2000 with TBS-T buffer. The membranes were washed with TBS-T buffer and incubated with a goat anti-rabbit secondary antibody (1:10000; #56j9958, Affinity) for one hour. The positive bands were detected by enhanced chemiluminescence (ECL) using the ECL kit (biosharp), per the manufacturer's instructions.

Immunofluorescence

The adherent cells were fixed with 4% paraformaldehyde and incubated overnight with the anti-PMEL17 antibody (#sc-377325, SCBT), followed by fluorescent secondary antibodies (#S0005, Affinity). After counterstaining with DAPI (#BS097, Biosharp), the cells were observed under a confocal fluorescence microscope (LSM800; Zeiss, Oberkochen, Germany). The melanosomes with emitting red fluorescence were counted.

Quantitative reverse transcription-polymerase chain reaction (qRT-PCR)

The total cellular RNA was extracted using Fast total RNA extraction kit (FASTAGEN, Shanghai, China), and reverse-transcribed into cDNA using a reverse transcription kit (#R223-01, Vazyme), as per manufacturer's instructions. The SYBR green qPCR Mix (#11184ES08, YEASEN) was used, and the reaction was performed on a real-time PCR instrument (Roche Light Cycler 480II, Basel, Switzerland). *GAPDH* was used as the internal control. The relative expression levels of *MITF*, *TYR*, *TYRP1*, *DCT*, *RAB27A*, *MYO5A*, *VEGF*, *PTGS2*, *FGF2*, *ET-1*, *WNT3*, *WNT7A*, *TRPV1*, *TRPV2*, *TRPV3*, and *TRPV4*, were calculated according to the Δ Ct formula and normalized against *GAPDH* housekeeping gene. The primer sequences are listed in [Table S1](#).

Human skin samples

Approved by the Ethics Committee of the Third Xiangya Hospital of Central South University and with the consent of the donors, skin tissue samples were collected from male adolescent circumcision in the Department of urology in the Third Xiangya Hospital of Central South University. In addition, the Erythema Ab Igne (EAI) specimens were donated by patients of the dermatology department of the Third Xiangya Hospital of Central South University. The foreskins were cut into pieces and carefully placed in DMEM (#C11995500BT, Gibco, NY) supplemented with 20% or 10% FBS (Biological Industries, Israel) and 1% penicillin-streptomycin (#ABT920, G-CLONE) antibiotic mixture. The skin pieces were allowed to float on the medium, with the epidermis facing up at the air/liquid interface and the dermis/subcutis facing down. The tissues were cultured at 37°C in a humidified CO₂ incubator containing 5% CO₂ and kept for 5 days, and exposed to different temperatures (37°C, 39°C and 41°C) every day for 1 hour.

Immunohistochemistry

The paraffin sections were deparaffinized, cleared with xylene, and hydrated through an ethanol gradient. After washing once with (Phosphate buffered saline) PBS, the slides were immersed in hot sodium citrate solution to retrieve antigens. The slides were then rinsed once with PBS, incubated with an endogenous

peroxidase blocking agent at room temperature for 10 min, and washed thrice with PBS. The sections were then blocked with 5% BSA for 30 min and incubated overnight with anti-PTCH1 (1:100; #A0826, ABclonal) and anti-GLI1 (1:150; #A14675, ABclonal) antibodies at 4°C. The following day, the slides were washed with PBS and then incubated with 100µL of a reaction enhancement solution at room temperature for 20 min. The slides were then washed thrice with PBS, incubated with HRP-labeled goat anti-rabbit IgG antibody at 37°C for 30 min, washed thrice with PBS, developed with 3,3'-diaminobenzidine (DAB) substrate, and counterstained with hematoxylin. After dehydrating with an ethanol gradient and clarification with xylene, the specimens were sealed with a neutral resin and observed under an inverted microscope.

Cytoplasmic Ca²⁺ measurement

The suitably treated cells were incubated with 2µM Fluo-4-AM (#S1060, Beyotime) for 40 min. The reaction mixture was diluted by adding PBS, and the cells were left undisturbed for 25 min. The intensity of green fluorescence corresponding to cytoplasmic Ca²⁺ level was determined by confocal microscopy (LSM800; Zeiss, Oberkochen, Germany).

RNA high-throughput sequencing

RNA was extracted from HaCaT cells and cultured in the medium at 41°C for 3 days, and RNA sequencing was performed using the Illumina platform per the manufacturer's instructions. Three biological replicates were analyzed for each group.

QUANTIFICATION AND STATISTICAL ANALYSIS

All values are presented as mean ± SD and data were obtained from three independent experiments. Statistical analyses were performed on individual experiments, as indicated, with GraphPad Prism 9.0 software using an unpaired t-test, equal variance for comparison between two groups and one-way ANOVA for comparisons between more than two groups. A *P* value of **P*<0.05 was considered as statistically significant.